Available online at www.sciencedirect.com
ScienceDirect
Journal of Power Sources 172 (2007) 410–415
JOURNAL OF POWER SOURCES
www.elsevier.com/locate/jpowsour

Short communication

Synthesis of spinel $LiMn_2O_4$ nanoparticles through one-step hydrothermal reaction

C.H. Jiang [a,b,*], S.X. Dou [b], H.K. Liu [b], M. Ichihara [c], H.S. Zhou [a,**]

[a] *Energy Technology Research Institute, National Institute of Advanced Industrial Science and Technology, Umezono 1-1-1, Tsukuba, Ibaraki 305-8568, Japan*
[b] *Institute for Superconducting and Electronic Materials, University of Wollongong, Northfields Avenue, Wollongong, NSW 2522, Australia*
[c] *Institute for Solid State Physics, The University of Tokyo, Kashiwanoha, Kashiwa, Chiba 277-8581, Japan*

Received 6 June 2007; received in revised form 18 July 2007; accepted 23 July 2007
Available online 27 July 2007

Abstract

Phase pure spinel $LiMn_2O_4$ nanoparticles can be directly synthesized by one-step hydrothermal reaction of γ-MnO_2 with LiOH in an initial Li/Mn ratio of 1 at 200 °C. The reaction might involve a redox reaction between Mn^{4+} and OH^-, and the formation of $LiMn_2O_4$ at the same time under the proposed hydrothermal conditions. This hydrothermal process is simple since only γ-MnO_2 powders are used as the Mn source, whereas without use of any oxidants, reductants, or low valence Mn source. The electrochemical performance of the as-synthesized $LiMn_2O_4$ nanoparticles towards Li^+ insertion/extraction was examined. Rather good capacity and cycle performance, and an especially excellent high rate capability, were observed for the sample that was hydrothermally reacted for 3 days.

Keywords: Spinel $LiMn_2O_4$; Hydrothermal synthesis; Li-ion batteries; Rate capability

1. Introduction

Li-ion batteries are the major power sources of today's portable electronic devices and also possibly for future electric vehicles, provided that the power and energy densities could be further improved. The positive electrode material of commercialized Li-ion batteries is $LiCoO_2$, which has many disadvantages, such as toxicity, cause of exposure, scare raw materials, and high price. Alternative positive electrode materials, such as $Li(Ni,Mn,Co)O_2$, $LiMn_2O_4$, $LiFePO_4$, Li_2FeSiO_4, and so on, have been proposed as replacements. Among these materials, spinel $LiMn_2O_4$ has attracted special interest because of its significant advantages over $LiCoO_2$ in terms of its non-toxicity, safety, and abundant raw materials [1,2]. Regarding this material, a large amount of work involving the synthesis, Li insertion/extraction mechanism, element substitution, and electrochemistry have been done in order to facilitate its practical applications [3–7]. In general, the electrochemical performance of $LiMn_2O_4$ is intimately related to its phase purity, crystallinity, particle size, and morphology [8]. All of these aspects can be correlated to the materials synthesis. Conventionally, spinel $LiMn_2O_4$ was prepared by solid-state reaction of manganese oxides, nitrate or carbonate with lithium hydroxide, nitrate or carbonate at temperatures as high as 700–900 °C [1–8]. The final products usually contain large irregular particles with a broad size distribution, as well as impurity phases. Also, it is difficult to control the crystalline growth, compositional homogeneity, morphology, and microstructure. Some soft chemistry routes, such as sol–gel [9,10], Pechini [11], emulsion [12], melt-impregnation [13], spray-drying [14], etc., have also been proposed. These methods lead to homogeneous spinel materials with smaller particle size. However, these methods also suffered from high temperature heat treatment, use of expensive reagents, and process complexity.

In recent years, the hydrothermal method has been demonstrated as an attractive low temperature route to prepare crystalline spinel $LiMn_2O_4$ [15–19]. However, the proposed

* Corresponding author at: Energy Technology Research Institute, National Institute of Advanced Industrial Science and Technology, Umezono 1-1-1, Tsukuba, Ibaraki 305-8568, Japan.
** Corresponding author.
E-mail addresses: chunhai_jiang@yahoo.com (C.H. Jiang), hs.zhou@aist.go.jp (H.S. Zhou).

0378-7753/$ – see front matter © 2007 Elsevier B.V. All rights reserved.
doi:10.1016/j.jpowsour.2007.07.039

hydrothermal processes have more or less disadvantages. For example, in some processes, other oxidants, reductants, or low valence Mn source, such as H_2O_2, glucose, or $Mn(NO_3)_2$, have to be used together with the manganese sources to first obtain mixed valences of Mn^{4+} and Mn^{3+} in the starting materials, which lead to the process complexity. Feng et al. [15] reported a simple process without using additional reagents other than γ-MnO_2 and LiOH, but their process involved a very long hydrothermal treatment of 24 days, possibly due to the low reaction temperature (170 °C), and low initial Li/Mn ratio (<0.5). Also, we noticed that the results for a similar hydrothermal synthesis were very controversial from authors to authors. For example, for a hydrothermal treatment at 180 °C for 96 h with Li/Mn = 1, Li et al. [20] only obtained γ-MnO_2 nanowires, but Qian et al. [21] obtained spinel $LiMn_2O_4$. These controversial results suggest that a systematic study on the hydrothermal synthesis of spinel $LiMn_2O_4$ is still necessary. In this paper, we report a simple hydrothermal process, in which low grade γ-MnO_2 was used as the single Mn source, which hydrothermally reacted with LiOH aqueous solution at 200 °C under autogenetic pressure to form well-crystallized nanocrystalline spinel $LiMn_2O_4$. The reaction mechanism, structure, morphology, and electrochemical performance of the synthesized spinel $LiMn_2O_4$ nanopowders were systematically studied.

2. Experimental

Spinel $LiMn_2O_4$ powders were hydrothermally synthesized directly from γ-MnO_2 and LiOH aqueous solution without any additional reagents. In a typical process, 1.5 mmol $LiOH{\cdot}H_2O$ (98–102%, Wako, Japan) was dissolved in 35 ml distilled water. To this solution, 1.5 mmol low grade γ-MnO_2 (≥90%, Soekawa Chemicals, Japan) was added to make the Li/Mn ratio equal to 1. The resulting slurry was magnetically stirred for 30 min, and then was transferred into a Teflon-lined autoclave with a volume of 45 ml. The tightly sealed autoclave was kept at 200 °C for 1–7 days in an oven. After the hydrothermal treatment, the products were separated by suction-assisted filtration, washed with distilled water and absolute ethanol several times, and then dried in air at 70 °C for several hours.

X-ray diffraction (Cu Kα, λ = 1.5406 Å), scanning electron microscopy (SEM) and transmission electron microscopy (TEM) were used to characterize the as-prepared $LiMn_2O_4$ powders. The electrochemical performance of the as-prepared powders was investigated with a beaker-type three-electrode cell. The working electrode was composed of 70% $LiMn_2O_4$, 20% acetylene black (AB) carbon and 10% Teflon (poly(tetrafluoroethylene)) binder by weight. Li metal was used as the counter and reference electrodes. The electrolyte was 1 M $LiClO_4$ in ethylene carbonate (EC) and diethyl carbonate (DEC) (EC/DEC = 1/1, v/v). Galvanostatic charge/discharge measurements were performed within a potential range of 3.0–4.5 V versus Li/Li^+. The specific capacity and current density were based on the active material ($LiMn_2O_4$) only, which was typically 4–5 mg cm^{-2}. Cyclic voltammograms were recorded at a scan rate of 0.1 mV s^{-1} within 3.1–4.5 V versus Li/Li^+.

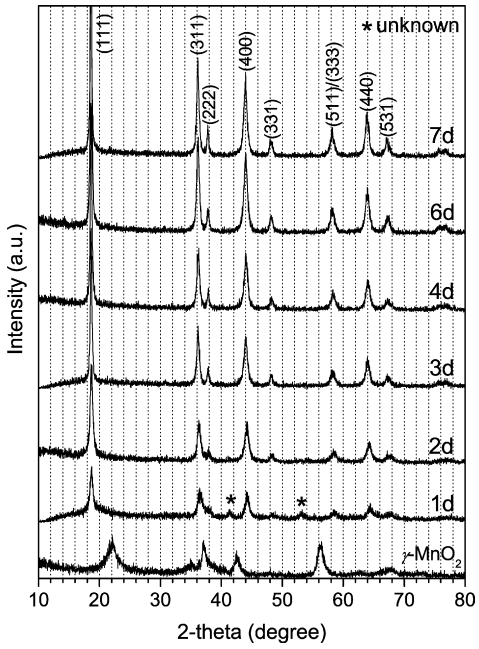

Fig. 1. The XRD patterns of the starting γ-MnO_2 powders and the $LiMn_2O_4$ products obtained by hydrothermal reaction of γ-MnO_2 and LiOH for different periods of time at 200 °C.

3. Results and discussion

Fig. 1 shows the XRD patterns of the starting γ-MnO_2 powders and the $LiMn_2O_4$ products prepared by hydrothermal reaction of γ-MnO_2 and LiOH for different periods of time. As can be seen, the starting γ-MnO_2 disappeared after 1 day of hydrothermal reaction. Besides some weak unidentified peaks, the main XRD peaks of this sample can be indexed to $LiMn_2O_4$, although the peak positions are slightly shifted to higher 2θ angle. As reaction time increased, the phase purity, peak intensity and crystallinity of the products were gradually improved. Meanwhile, the peaks were shifted to lower 2θ angles, resulting in a perfect match of the XRD patterns of the sample reacted for 7 days with that of the standard data, JCPDS no. 35-0782. It is evident that spinel $LiMn_2O_4$ has been successfully synthesized by the one-step hydrothermal reaction under the current conditions, i.e., at 200 °C and with Li/Mn = 1. Compared to the previous proposed hydrothermal processes [16–19], the present process is very simple, since no any other oxidants, reductants, or low valence Mn source are added. Also, the current process is much faster than the one proposed by Feng et al. [15]. It is supposed that the higher Li/Mn ratio and higher temperature in our experiments might be the major reasons for this faster synthesis of $LiMn_2O_4$.

To clarify the controversial reports in literatures, several parameters, including the starting powders, temperature, Li/Mn ratio, and reaction time, were also tested in our hydrothermal synthesis. It was found that there was no observable difference between the products when using either low grade γ-MnO_2 or high purity (99%) electrolytic manganese dioxide (EMD) as starting powders. An initial Li/Mn ratio of 1 was found to be one of the key parameters to the synthesis of $LiMn_2O_4$. At a lower

Li/Mn ratio, such as 0.75, phase pure $LiMn_2O_4$ could not be obtained after 3 days reaction at 200 °C. Increasing the Li/Mn ratio to 2 or higher would lead to the formation of Li_2MnO_3 together with $LiMn_2O_4$. Regarding the reaction temperature, if the hydrothermal synthesis was carried out at 180 °C while keeping Li/Mn = 1, only γ-MnO_2 nanowires were obtained after 4 days of treatment, consistent with the recent report of Li et al. [20]. This indicates that the reaction temperature of 200 °C is crucial for the hydrothermal synthesis of $LiMn_2O_4$ in our study.

The lattice parameter, a_0, of the obtained spinel $LiMn_2O_4$ powders was calculated from the XRD data using Unitcell software, see Fig. 2. At first, a_0 increased dramatically from 8.180 Å (1 day) to 8.223 Å (3 days). Then, it increased slightly to 8.226 Å up to 6 days. After being reacted for 7 days, a_0 increased to 8.241 Å, close to the standard data, $a_0 = 8.247$ Å, of JCPDS no. 35-0782. The ideal spinel structure (space group *Fd*3*m*) can be described as consisting of a cubic close-packing arrangement of oxygen ions at the 32e sites, the Li^+ ions at the tetrahedral (8a) sites, and the Mn^{4+} and Mn^{3+} ions at the octahedral (16d)

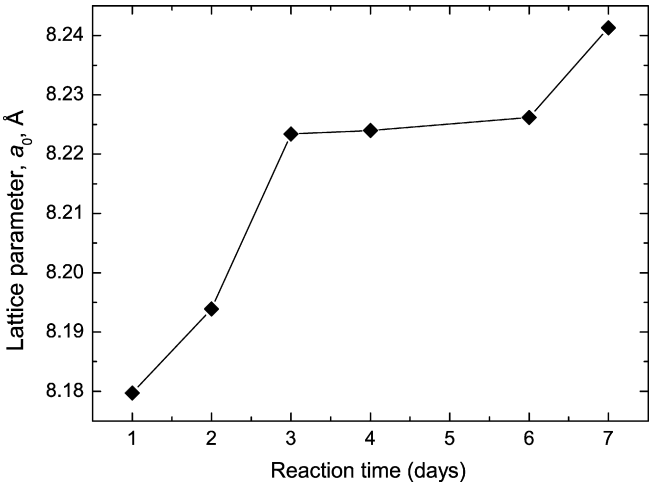

Fig. 2. The lattice parameter, a_0, of the as-synthesized $LiMn_2O_4$ powders as a function of reaction time.

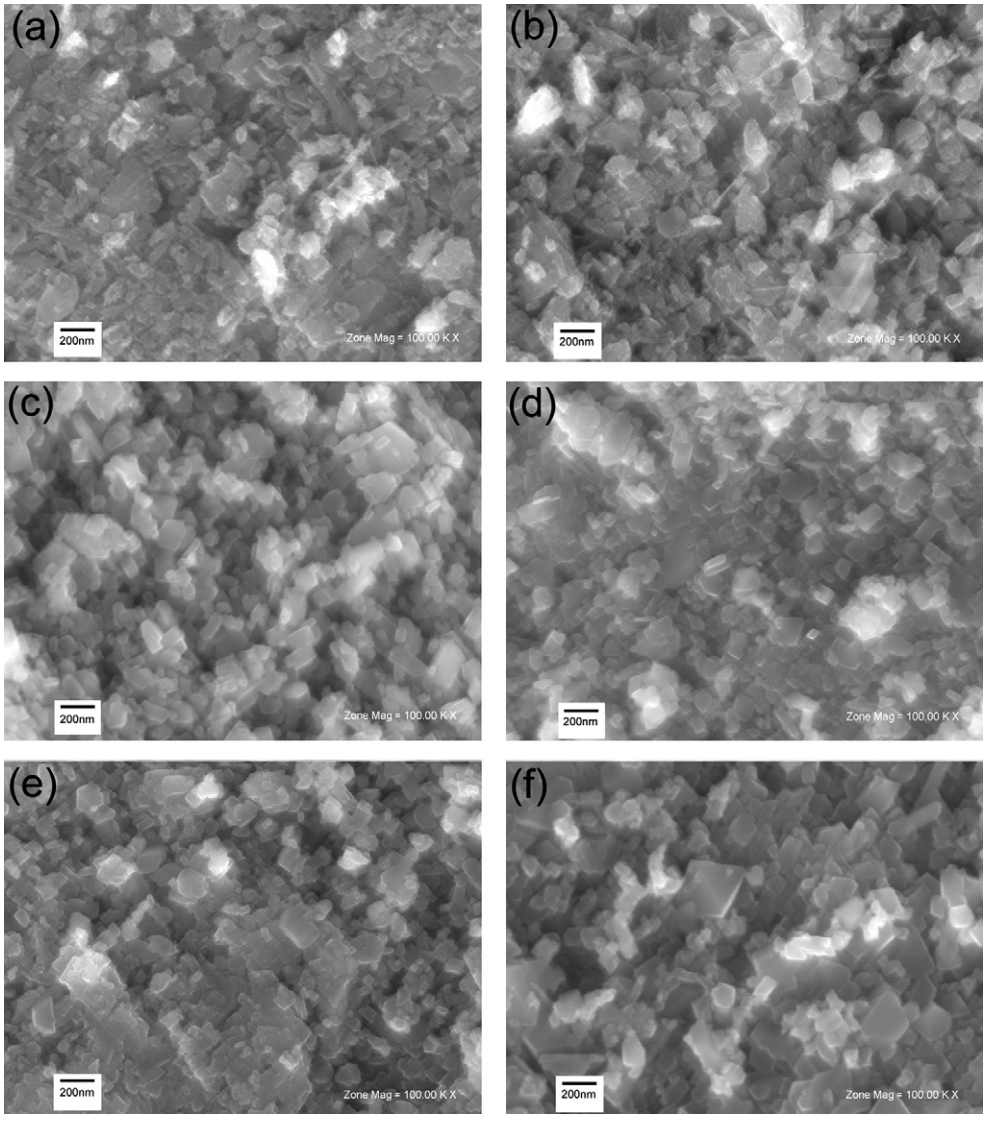

Fig. 3. SEM images of the starting γ-MnO_2 powders (a) and the as-synthesized $LiMn_2O_4$ products after a reaction time of 1 day (b), 3 days (c), 4 days (d), 6 days (e) and 7 days (f).

sites [4,5,22]. The average oxidation state of manganese in the ideal spinel $LiMn_2O_4$ is 3.5, namely, the $Mn^{3+}$and Mn^{4+} ions occupy half of the 16d sites, respectively. From Figs. 1 and 2 we know that an ideal spinel structured $LiMn_2O_4$ has been formed after the hydrothermal treatments of 7 days. This indicates that a redox reaction must have occurred during the hydrothermal synthesis, leading to the reduction of half of the Mn^{4+} ions to the Mn^{3+} ions.

Based on the above analysis, the possible chemical reaction in the synthesis of $LiMn_2O_4$ under the proposed hydrothermal conditions might be as follows:

$$4LiOH + 8MnO_2 \rightarrow 4LiMn_2O_4 + 2H_2O + O_2\uparrow \quad (1)$$

According to this reaction, Mn^{4+} ions were reduced by OH^-, leading to mixed valences of Mn^{4+}/Mn^{3+} in the reaction system. Oxygen was released as the result of oxidation of OH^- by Mn^{4+}. This reaction is different from the previously proposed ones [15–19]. The reduction of Mn^{4+} and formation of $LiMn_2O_4$ might be carried out simultaneously. Any pre-treatment of the Mn^{4+} ions by adding reductants or low valence Mn^{2+} to get mixed Mn^{4+}/Mn^{3+} ions was eliminated.

The evolution of a_0 with reaction time as shown in Fig. 2 can be used to track the reaction during the hydrothermal synthesis. At an early stage of $LiMn_2O_4$ formation, due to the lack of enough Mn^{3+} ions, some Li^+ ions would occupy the 16d sites, resulting in Li-rich $Li_{1+x}Mn_{2-x}O_4$ [5,22]. The a_0 was small due to the smaller ionic radii of Li^+ and Mn^{4+} as compared to Mn^{3+}. As the reaction proceeded, the number of Mn^{3+} ions increased as the number of Mn^{4+} ions decreased. Because of the larger ionic radius of Mn^{3+} (0.65 Å) compared to Mn^{4+} (0.53 Å) [23], a_0 increased dramatically. From 3 days to 6 days, a_0 only increased slightly, suggesting that reaction (1) was slowed down during this period possibly due to the reduced concentration of OH^-. At this stage, the products were still Li-rich, since some of the 16d sites were still occupied by Li^+ ions. According to the reports of Xia et al. [5], the estimated Li/Mn ratio was around 0.55 when the reaction time was less than 6 days, indicating Li-rich compositions. The reaction was completed after 7 days, which resulted in a_0 of 8.241 Å and a Li/Mn ratio close to 0.5, very similar to that of stoichiometric $LiMn_2O_4$.

Fig. 3 presents the microstructural morphologies of the starting γ-MnO_2 powders (a) and the $LiMn_2O_4$ products prepared by hydrothermal reaction for 1 day (b), 3 days (c), 4 days (d), 6 days (e), and 7 days (f), respectively. The starting γ-MnO_2 powders show irregular grains. The weak and broad XRD peaks shown in Fig. 1 indicate that the starting γ-MnO_2 powders have low crystallinity. After 1 day of hydrothermal treatment, the sample still showed irregular grains. However, crystalline $LiMn_2O_4$ grains can be clearly seen. With increasing reaction time, the crystallinity of the $LiMn_2O_4$ powders was further improved, which was consistent with the increase in the intensities of the XRD peaks as shown in Fig. 1. For the sample hydrothermally treated for 7 days, well-defined single crystals with an octahedral shape were clearly observed, indicating that well-crystallized spinel $LiMn_2O_4$ nanoparticles had been successfully synthesized.

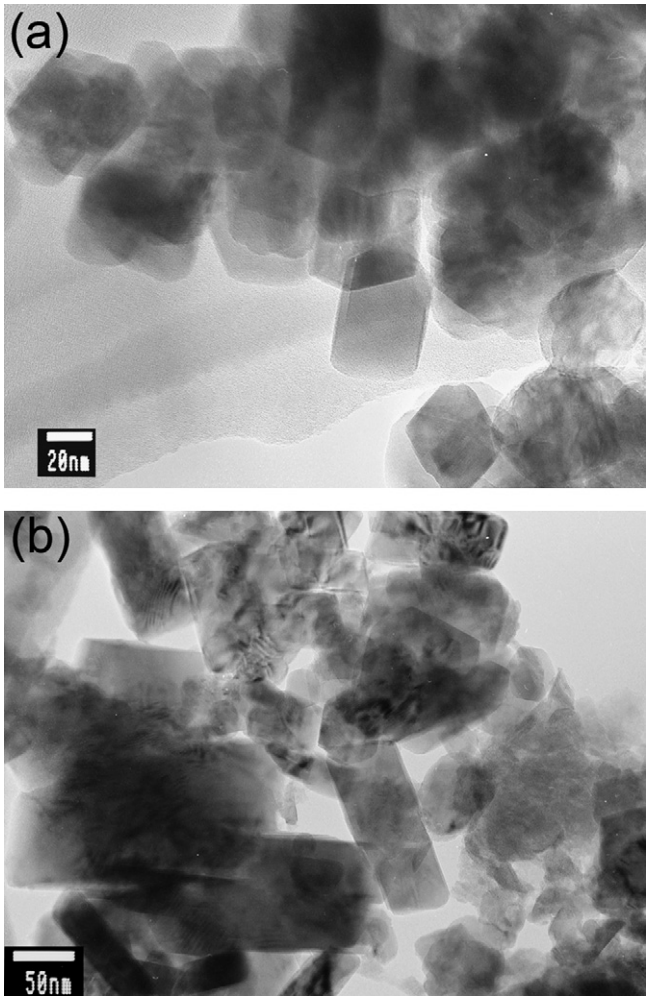

Fig. 4. TEM images of $LiMn_2O_4$ powders after a reaction time of 3 days (a) and 6 days (b).

Fig. 4(a) and (b) show the TEM images of the $LiMn_2O_4$ powders hydrothermally treated for 3 and 6 days, respectively. As can be seen, the typical size of the $LiMn_2O_4$ grains was around 30 nm for the sample treated for 3 days, but 50 nm for the sample treated for 6 days. This was also consistent with the sharpening of the XRD peaks with increasing reaction time, i.e., increasing the reaction time had promoted the grain growth.

The electrochemical behaviors of Li^+ insertion/extraction into/from the as-synthesized $LiMn_2O_4$ nanoparticles were evaluated by cyclic voltammograms (CV) within the potential range between 3.1 and 4.5 V versus Li/Li^+ at a scan rate of 0.1 mV s^{-1}. Fig. 5 shows the CV curves of selected cycles of the samples hydrothermally treated for 3 days (a) and 6 days (b), respectively. Two pairs of prominently separated redox peaks, which were located at around the potentials of 4.02 and 4.15 V (anodic) and 3.97 and 4.09 V (cathodic), were observed in both figures, which were typical for spinel $LiMn_2O_4$. The well-defined CV curves provided another piece of evidence that nanosized spinel $LiMn_2O_4$ powders with high crystallnity and electroactivity have been successfully fabricated.

The specific capacities of the hydrothermal products at different current rates were determined by galvanostatic

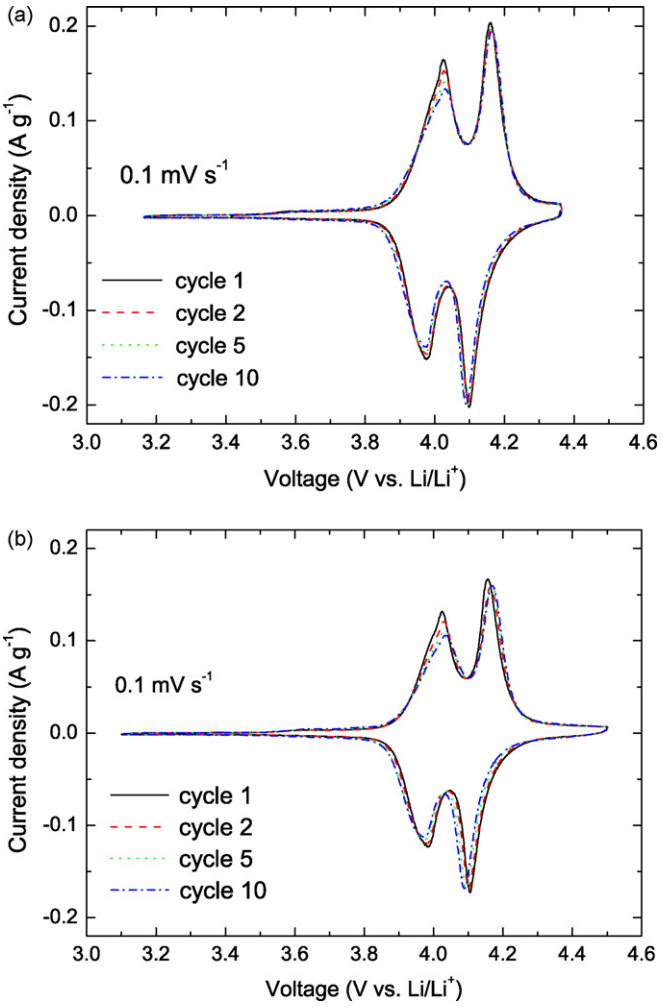

Fig. 5. Cyclic voltammograms of the samples hydrothermally treated for 3 days (a) and 6 days (b). The scan rate is 0.1 mV s^{-1}.

charge/discharge measurements between the cutoff voltages of 3.0 and 4.5 V versus Li/Li^+. The cells were first charged to 4.5 V (vs. Li/Li^+) before the subsequent discharge/charge measurements. Fig. 6 shows the second cycle charge and discharge curves at 0.1, 1 and 2 A g^{-1} for the samples produced by 3 and 6 days of hydrothermal treatments. At 0.1 A g^{-1}, even at 1 A g^{-1}, a two-stage electrochemical Li^+ insertion/extraction behavior was clearly observed in both samples, which is characteristic for spinel $LiMn_2O_4$, and was also consistent with the CV curves as shown in Fig. 5. As seen from Fig. 6, these two samples showed similar charge capacities (110 mAh g^{-1}) and discharge capacities (108.3 mAh g^{-1}) at 0.1 A g^{-1}. However, at higher current rates, the sample treated for 3 days showed obviously higher capacities than that treated for 6 days. For example, the charge and discharge capacities of the former were 81.4 and 79.4 mAh g^{-1} at 2 A g^{-1} (~16*C* if $1C = 120$ mA g^{-1}), respectively; whereas these values were only 65 and 62.7 mAh g^{-1} for the latter. This indicates that the sample treated for the shorter time had better high rate performance. As discussed above, the sample hydrothermally treated for 6 days shows higher crystallinity, but also a larger grain size, than that treated for only 3 days. Generally, higher

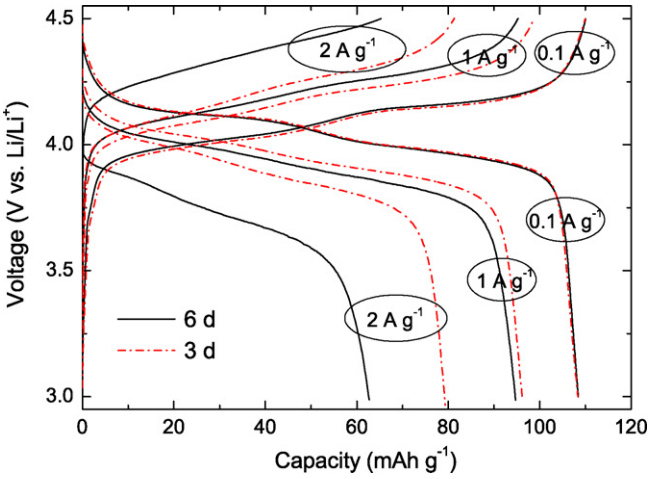

Fig. 6. Charge and discharge curves at different current densities for the samples obtained by hydrothermal reaction for 3 and 6 days.

crystallinity and smaller grain size may correspond to higher capacity and better high rate property [8]. The results shown in Fig. 6 indicated that a smaller grain size might have played a more important role in the high rate performance of nanosized $LiMn_2O_4$.

The cycling performances (discharge capacities) at different current rates of the two samples discussed in Fig. 6 are given in Fig. 7. Both samples show high cycle stability under the measured current densities, especially the one hydrothermally treated for 3 days. A discharge capacity of 91 mAh g^{-1} was maintained after 100 cycles at 1 A g^{-1} (8*C*), which was 95.7% of the initial discharge capacity. At 2 A g^{-1}, the capacity retention ratio decreased a little; however, after 100 cycles, about 86% of the initial discharge capacity was still preserved in this sample. The data presented in Figs. 6 and 7 were much better than most of the reported results for nanosized $LiMn_2O_4$ [16,24–26], which strongly suggested that the current simple hydrothermal process had produced high quality nanosized $LiMn_2O_4$ powders in term of rate capability and cycle stability.

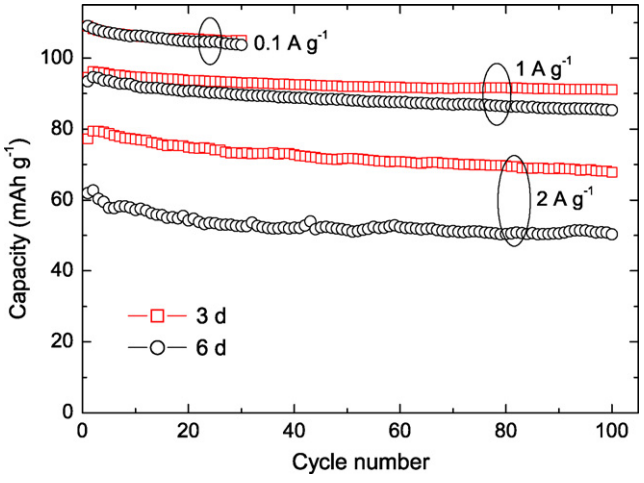

Fig. 7. Cycle performances at different current densities of the two samples presented in Fig. 6.

4. Conclusion

A simple one-step hydrothermal reaction process was developed to synthesize nanostructured $LiMn_2O_4$ cathode material. Low grade γ-MnO_2 and LiOH with a molar ratio of 1:1 can hydrothermally react at 200 °C to form well-crystallized $LiMn_2O_4$ nanoparticles in a relatively short period of time. The process is very simple, since the hydrothermal reaction only involves the redox reaction between Mn^{4+} and OH^-, without the addition of any oxidants, reductants, or lower valence Mn source, as was done in previous reports. The as-prepared $LiMn_2O_4$ nanoparticles showed rather good capacity and cycle performance, and an especially excellent high rate capability for the sample hydrothermally reacted for 3 days.

References

[1] D. Guyomard, J.M. Tarascon, J. Electrochem. Soc. 138 (1991) 2864.
[2] J. Kim, A. Manthiram, Nature 390 (1997) 265.
[3] J.M. Tarascon, M. Armand, Nature 414 (2001) 359.
[4] Y. Xia, M. Yoshio, J. Electrochem. Soc. 143 (1996) 825.
[5] Y. Xia, Y. Zhou, M. Yoshio, J. Electrochem. Soc. 144 (1997) 4186.
[6] T. Ohzuku, M. Kitagawa, T. Hirai, J. Electrochem. Soc. 137 (1990) 769.
[7] S. Soiron, A. Rougier, L. Aymard, J.M. Tarascon, J. Power Sources 97/98 (2001) 402.
[8] R. Alcantara, P. Lavela, P.L. Relano, J.L. Tirado, E. Zhecheva, R. Stoyanova, Inorg. Chem. 37 (1998) 264.
[9] S. Bach, M. Henry, N. Baffier, J. Livage, J. Solid State Chem. 88 (1990) 325.
[10] J.H. Choy, D.H. Kim, C.W. Kwon, S.J. Hwang, Y.I. Kim, J. Power Sources 77 (1999) 1.
[11] W. Liu, G.C. Farrington, F. Chaput, B. Dunn, J. Electrochem. Soc. 143 (1996) 879.
[12] S.T. Myung, H.T. Chung, J. Power Sources 84 (1999) 32.
[13] Y. Xia, H. Takeshige, H. Noguchi, M. Yoshio, J. Power Sources 56 (1995) 61.
[14] H.M. Wu, J.P. Tu, Y.F. Yuan, Y. Li, X.B. Zhao, G.S. Cao, Scripta Mater. 52 (2005) 513.
[15] Q. Feng, H. Kanoh, Y. Miyai, K. Ooi, Chem. Mater. 7 (1995) 1226.
[16] Y.Y. Liang, S.J. Bao, B.L. He, W.J. Zhou, H.L. Li, J. Electrochem. Soc. 152 (2005) A2030.
[17] Y.C. Zhang, H. Wang, H.Y. Xu, B. Wang, H. Yan, A. Ahniyaz, M. Yoshimura, Solid State Ionics 158 (2003) 113.
[18] K. Kanamura, K. Dokko, T. Kaizawa, J. Electrochem. Soc. 152 (2005) A391.
[19] H.M. Wu, J.P. Tu, Y.F. Yuan, X.T. Chen, J.Y. Xiang, X.B. Zhao, G.S. Cao, J. Power Sources 161 (2006) 1260.
[20] G.C. Li, L. Jiang, H.T. Pang, H.R. Peng, Mater. Lett. 61 (2007) 3319.
[21] X.L. Li, R.M. Xiang, T. Su, Y.T. Qian, Mater. Lett. 61 (2007) 3591.
[22] A. de Kock, M.H. Rossouw, L.A. de Picciontto, M.M. Thackeray, W.I.F. David, R.M. Ibberson, MRS Bull. 25 (1990) 657.
[23] R. Premanand, A. Durairajan, B. Haran, R. White, B. Popov, J. Electrochem. Soc. 149 (2002) A54.
[24] L.I. Hill, R. Portal, A.L.G.L. Salle, A. Verbaere, D. Guyomard, Electrochem. Solid-State Lett. 4 (2001) D1.
[25] V.G. Kumar, J.S. Gnanaraj, S.B. Dacid, D.M. Pickup, E.H. van-Eck, A. Gedanken, D. Aurbach, Chem. Mater. 15 (2003) 4211.
[26] X. Li, F. Cheng, B. Guo, J. Chen, J. Phys. Chem. B 109 (2005) 14017.